Mechanism-Based Thrombin Inhibitors: Design, Synthesis, and Molecular Docking of a New Selective 2-Oxo-2*H*-1-benzopyran Derivative

Raphaël Frédérick,*[,†,‡] Séverine Robert,[†] Caroline Charlier,[§] Johan Wouters,[§] Bernard Masereel,[†] and Lionel Pochet[†]

Department of Pharmacy and CBS Laboratory, Drug Design and Discovery Center (D3C), University of Namur, FUNDP, 61, Rue de Bruxelles, B-5000 Namur, Belgium

Received November 27, 2006

New 2-oxo-2*H*-1-benzopyran derivatives were prepared to optimize **2a**,**b**, initially developed as mechanism-based α-chymotrypsin (α-CT) inhibitors, into potent and selective thrombin (THR) inhibitors. From this study, **22**, characterized by a 2-(*N*-ethyl-2′-oxoacetamide)-5′-chlorophenyl ester side chain, was shown to be a good THR inhibitor (k_i/K_I = 3455 $M^{-1}\cdot s^{-1}$), displaying an excellent selectivity profile against other serine proteases such as factor Xa, trypsin, and α-CT. Docking analysis of this compound into the different protein structures revealed the molecular basis responsible for its potency and selectivity.

Introduction

Thrombin (THR) is a key enzyme involved in the last step of the coagulation cascade. By converting the glycoprotein fibrinogen into fibrin monomers, THR is responsible for clot stabilization and therefore plays a major role in hemostasis and thrombosis. In addition, this enzyme is one of the most potent stimulators of platelet secretion and aggregation. THR is thus clearly recognized as an attractive target for the development of inhibitors in thrombotic disorders.[1,2]

Most THR inhibitors designed up to now bind the enzyme through formation of a salt bridge between Asp189 at the bottom of the specificity pocket (S1 or S pocket) and a positively charged group in the P1 position of the ligand.[1] Recently, different groups have shown that THR inhibitors deprived of such a basic moiety demonstrate improved bioavailability and pharmacokinetics.[3−8] In this context, Merck has reported **1a**, characterized by a 2′,5′-dichlorophenyl moiety, as one of the first potent nonbasic THR inhibitors.[8] The binding mode of this compound, revealed by X-ray diffraction, implicates a strong hydrophobic interaction between the chlorine in the 5′-position and the aromatic ring of Tyr228 deeply inserted within the S-pocket. Replacement of the 2′-chlorine by a 2-(*N*-ethyl-2′-oxoacetamide) moiety (**1b**) further improved the potency and the solubility in comparison to **1a**.

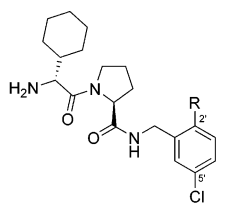

		K_i (THR) (nM)
1a	R = Cl	5
1b	R = $OCH_2CONHEt$	0.74

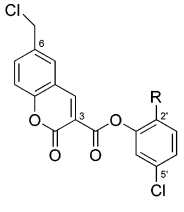

		K_i/K_I (THR) ($M^{-1}s^{-1}$)	K_i/K_I (α-CT) ($M^{-1}s^{-1}$)
2a	R = H	7,720	762,700
2b	R = Cl	37,000	220,000

In this context, our group has recently reported that coumarins, initially developed as mechanism-based α-chymotrypsin (α-CT) inhibitors,[9] were also potent nonbasic THR inhibitors.[10] In particular, **2a**, strongly active on α-CT (k_i/K_I = 762 700 $M^{-1}\cdot s^{-1}$), displays an interesting inhibitory potency against THR, with inhibitory parameters k_i/K_I of 7720 $M^{-1}\cdot s^{-1}$.[9,10] Introduction of a chlorine in the 2′-position (**2b**) enhanced THR inhibition (k_i/K_I = 37 000 $M^{-1}\cdot s^{-1}$) about 5-fold without really modifying the potency against α-CT (k_i/K_I = 220 000 $M^{-1}\cdot s^{-1}$).

Taking advantage of the structure−activity relationships (SAR) described by Merck for **1a**,**b**, we aimed to optimize coumarins **2a**,**b** into more potent and selective THR inhibitors. In this paper, we thus report the development of new coumarins characterized by a 2′-substituted 5′-chlorophenyl side chain linked to the coumarin ring in the 3-position by an ester, methyl ester, or an amide. To rationalize the SAR and selectivity observed, a molecular docking study was efficiently realized using the automated GOLD docking software.

Chemistry

Targeted compounds **21**−**29** were prepared by reaction between the acid chloride and the appropriate amine or alcohols following the previously reported method.[9,10] However, this protocol required the prior synthesis of intermediates **4**, **7**, and **11** (Schemes 1 and 2). The 2-hydroxymethyl-4-chlorophenol **4** was obtained by reduction of the corresponding acid **3** with $LiAlH_4$ in THF (Scheme 1). The phenol **7** was prepared from **4** in three steps (Scheme 1): (a) **4** reacted with TBDMSCl in the presence of DMAP to give the silyl ether **5**, this latter being (b) alkylated with α-bromoacetic acid ethyl ester in dioxane and (c) deprotected with tetra-*N*-butylammonium fluoride in THF to afford the desired intermediate **7**.

The hydroxyl compound **11** was obtained from 2-methoxy-4-chlorophenol **8** (Scheme 2). This latter compound was first alkylated using α-bromoacetic acid ethyl ester and cesium carbonate in dioxane and then demethylated with boron tribromide. This reaction, accompanied by hydrolysis of the ester, led to acid **10**, which reacted with ethylamine in the presence of HOBT, NMM, and EDC in anhydrous DMF to give the targeted intermediate **11**.

Some 6-phenoxycoumarins have also been prepared. The intermediate 6-phenoxy-2-oxo-2*H*-1-benzopyrane-3-carboxylic acid **15** was synthesized according to Scheme 3. First, the 4-phenoxyphenol **12** reacted according to a Reimer−Tiemann reaction with chloroform and sodium hydroxide in an ethanolic/aqueous solution to afford the 2-hydroxy-5-phenoxybenzalde-

* To whom correspondence should be addressed. Phone: +32 (0)81 72 42 99. Fax: +32 (0)81 72 42 99. E-mail: raphael.frederick@gmail.com.
† Department of Pharmacy.
‡ Present address: Auckland Cancer Society Research Centre (ACSRC), University of Auckland, PO92319, Auckland, New Zealand.
§ CBS Laboratory.

10.1021/jm061368v CCC: $37.00 © 2007 American Chemical Society
Published on Web 06/20/2007

Scheme 1[a]

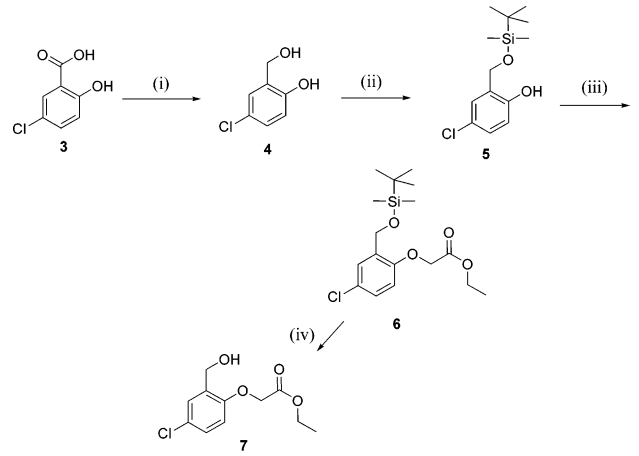

[a] Reagents and conditions: (i) $LiAlH_4$, THF, room temp, 16 h; (ii) TBDMSCl, NEt_3, DMAP, CH_2Cl_2, 0 °C → room temp, 2.5 h; (iii) $BrCH_2COOEt$, Cs_2CO_3, dioxane, room temp, 4 h; (iv) NBu_4F, THF, room temp, 1 h.

Scheme 2[a]

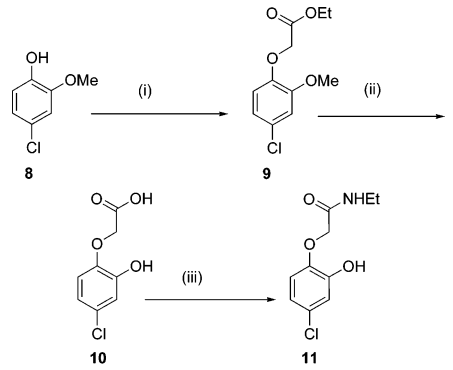

[a] Reagents and conditions: (i) $BrCH_2COOEt$, Cs_2CO_3, dioxane, room temp, 4 h; (ii) BBr_3, CH_2Cl_2, room temp, 1 h; (iii) $EtNH_2.HCl$, HOBt, NMM, EDC, DMF, room temp, 18 h.

Scheme 3[a]

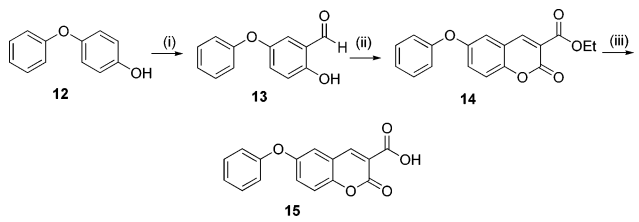

[a] Reagents and conditions: (i) $CHCl_3$, NaOH, H_2O, EtOH, reflux, 12 h; (ii) diethyl malonate, piperidine, HOAc, reflux, 14 h; (iii) NaOH, EtOH, H_2O, reflux, 1 h.

hyde **13**. This latter was then condensed with diethyl malonate under classical Knoevenagel conditions to give **14** and finally saponified to generate the desired acid **15**.

Finally, **4**, **7**, **11**, the 2,5-dichlorobenzyl alcohol **16**, 2,5-dichlorophenol **17**, 2,5-dichloroaniline **18**, and *N*-*tert*-butoxycarbonyl-2-hydroxy-4-chloroaniline **19** reacted with the acyl chloride of **15** or the 6-chloromethyl-2-oxo-2*H*-1-benzopyrane-3-carboxylic acid **20** obtained as previously described[9] to afford the targeted coumarins **21**−**29** (Table 1).

Results and Discussion

The inhibitory potency of **21**−**29** was first evaluated on isolated and purified THR. In this screening, the proteolytic activity of THR is measured 10 min after incubation with 100 μM inhibitor. For the drugs displaying high potency, lower concentrations were investigated. The results, displayed in Table 1, are expressed as the percentage of enzyme residual activity.

Table 1. Synthesis, Physicochemical Parameters, and in Vitro THR Residual Activity of Ester and Amide of 6-Chloromethyl- and 6-Phenoxycoumarins **21**−**29**

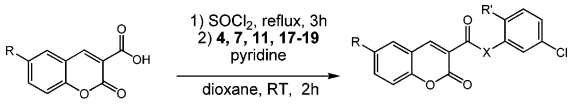

15-20 **2a-b, 21-29**

compd	R	X	R′	yield (%)	mp (°C)	[I] (μM)	THR residual activity (%)
2a[a]	CH_2Cl	O	H			2	10 ± 2
2b[a]	CH_2Cl	O	Cl			2	1 ± 0.1
21[b]	CH_2Cl	O	NH_2	55	254−258	100	60 ± 9
						100	6 ± 3
22	CH_2Cl	O	$OCH_2CONHEt$	15	124−127	10	3 ± 3
						2	11 ± 2
23	CH_2Cl	OCH_2	Cl	85	212−215	100	103 ± 4
24	CH_2Cl	OCH_2	OH	26	183−184	100	101 ± 1
25	CH_2Cl	OCH_2	OCH_2COOEt	38	134−136	100	95 ± 6
26	CH_2Cl	NH	Cl	39	281−282	100	91 ± 4
27	CH_2Cl	NH	OH	72	307[c]	100	110 ± 9
28	OPh	O	Cl	17	152−153	100	94 ± 6
29	OPh	O	H	31	119−122	100	90 ± 3

[a] From ref 10. [b] Obtained after deprotection of the amine using the mixture trifluoroacetic acid/CH_2Cl_2. [c] Decomposition.

Replacement of the 2′-chlorine atom of **2b** by an amine (**21**) greatly reduces THR inactivation potential (60% of THR residual activity at 100 μM vs 1% at 2 μM for **2b**). In contrast, introduction of a 2-(*N*-ethyl-2′-oxoacetamide) in this position leads to a good THR inhibitor (**22**) (11% of THR residual activity at 2 μM) as potent as **2a** (Table 1).

Compounds characterized by a benzyl ester (**23**−**25**) or a phenylamide (**26**, **27**) in the 3-position of the coumarin ring are all inactive. This emphasizes the importance of the ester linker to suitably orient the compounds in the enzyme active site (Table 1).

From a previous modeling study,[10] **2a**,**b** were shown to poorly occupy the D-pocket within the THR active site. On the basis of this observation, we designed **28** and **29**, analogous to **2a** and **2b**, respectively, and both are characterized by a phenoxy in the 6-position in place of a chloromethyl. The aromatic moiety might form an additional $\pi-\pi$ interaction with Trp215 inside the D-pocket, further stabilizing the compounds within the cleft. This modification, however, did not afford potent THR inhibitors. Indeed, up to now, all examples designed to replace the chloromethyl group led to inactive compounds. This result confirmed the importance of the CH_2Cl moiety in this series for the inhibition mechanism, as discussed later.

For the most active compound (**22**), a detailed enzymatic study was performed. The k_i/K_I ratio, which reflects the index of inhibitory potency for mechanism-based inhibitors,[11] was determined on THR but also on α-CT, factor Xa (FXa), and trypsin (TRY) to assess the selectivity of this compound against other serine proteases. The kinetic parameters k_i and K_I were determined using the progress curve or the preincubation method, depending on the protease.[12] In the progress curve method, the inhibitor competes with a chromogenic substrate to bind the enzyme. In the preincubation method, however, the enzyme and the inhibitor are incubated together before the determination of the remaining activity at regular time intervals. To assess the efficiency of our inhibitors, the partition ratio, defined as the ratio of product released to inactivation (k_{cat}/k_i), was also determined. The results are summarized in Table 2.

This study confirmed that **22** is a good THR inhibitor (k_i/K_I = 3455 $M^{-1}\cdot s^{-1}$, partition ratio of 13.5) even if slightly less

Table 2. Comparison of Kinetic Parameters k_i and K_I for Inactivation of THR, FXa, α-CT, and TRY by Derivatives **22** and **2a**,**b**

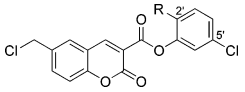

compd	R	THR k_i/K_I ($M^{-1}\cdot s^{-1}$)	THR k_{cat}/k_i	FXa k_{obs}/[I] ($M^{-1}\cdot s^{-1}$)	TRY k_{obs}/[I] ($M^{-1}\cdot s^{-1}$)	α-CT k_i/K_I ($M^{-1}\cdot s^{-1}$)	selectivity THR/α-CT
2a	H	7716 ± 952[a]	2.8	620 ± 36[a]	313 ± 55[a]	762700[b]	0.01
2b	Cl	37007 ± 5150[a]	1.8	219 ± 7[a]	685 ± 66[a]	288000[b]	0.13
22	*N*-ethyloxoacetamide	3457 ± 835	13.5	59 ± 2	118 ± 2	755 ± 45	5

[a] From ref 10. [b] From refs 9 and 13. Standard errors are less than 15%.

potent and efficient than **2a**,**b** ($k_i/K_I = 7720$ $M^{-1}\cdot s^{-1}$ and partition ratio of 2.8 for **2a**; $k_i/K_I = 37\,000$ $M^{-1}\cdot s^{-1}$ and partition ratio of 1.8 for **2b**) (Table 2). Of great interest, **22** was shown to exhibit a significantly improved selectivity against α-CT with a k_i/K_I of 755 $M^{-1}\cdot s^{-1}$ (vs 762 700 $M^{-1}\cdot s^{-1}$ for **2a** and 220 000 $M^{-1}\cdot s^{-1}$for **2b**). So **22** is about 5 times more potent on THR than on α-CT (selectivity ratio THR/α-CT of 5) compared to selectivity ratios of 0.01 and 0.13 for **2a** and **2b**, respectively. Furthermore, **22** is almost completely inactive on both FXa (k_{obs}/[I] = 60 $M^{-1}\cdot s^{-1}$, selectivity ratio THR/FXa of 58) and TRY (k_{obs}/[I] = 120 $M^{-1}\cdot s^{-1}$, selectivity ratio THR/TRY of 29).

The inhibition profile of **22** was further established on THR by enzymatic and mass spectrometry experiments, according to the well-established criteria for mechanism-based enzyme inactivators.[11] First, a typical saturation kinetic was observed for **22.** Second, the irreversibility of the THR inhibition by **22** was confirmed by ultracentrifugation experiments. Indeed, the inhibition was persistent even after removing the excess of inhibitor. Third, an enzyme−inhibitor complex with a 1:1 stoichiometry was obtained by mass spectrometry. A mass shift of 414 Da was observed between the THR−**22** complex (36 450.2 Da) and the native protein (36 036.2 Da) which corresponds to the exact mass of **22** (449 Da) less one chlorine atom. These findings confirm the mechanism-based behavior of **22** as already observed for these coumarin derivatives.[10] Details on these studies are given in the Supporting Information. To our knowledge, **22** constitutes a unique example of selective mechanism-based and nonbasic THR inhibitor.

Because all the serine proteases share the same catalytic mechanism, it is generally particularly difficult to achieve selectivity in mechanism-based inhibitors. To understand these results, i.e., the lower THR inhibitory potency of **22** compared to **2b** and its greatly improved selectivity profile, the binding modes of both compounds were investigated in the four serine proteases THR, α-CT, FXa, and TRY by molecular modeling.

The mechanism of inhibition proposed for these coumarins[14] implies the nucleophilic attack of the active Ser195 Oγ atom on the lactone carbonyl moiety. The resulting lactone ring opening leads to increased leaving properties of the 6-chlorine atom and the subsequent formation of an electrophilic quinone methide. This latter can then form a covalent bond with a nucleophilic residue, probably His57, within the active site. For this reaction to occur, the coumarin ring needs to be properly positioned in the neighborhood of Ser195; i.e., the lactone coumarin should be close to the hydroxyl group of Ser195 (distance of <3 Å).

Compounds **22** and **2b** were docked within the THR, FXa, α-CT, and TRY active sites using the automated GOLD program (PDB codes 1A4W, 1LPG, 4GCH, and 1EB2, respectively).[15] In each case, 100 conformations were produced and clustered by similarity. Two main modes were identified among the solutions: (i) the normal mode, which refers to the binding of the 2′-substituted 5′-chlorophenyl side chain within the S-pocket and the lactone coumarin close to the Ser195 residue and is the binding mode in agreement with the mechanism of inhibition described above and (ii) the inverse mode, which corresponds to the binding of the chloromethylcoumarin within the S-pocket and the lateral side chain outside the active site. Taking into account the protein flexibility, the conformations with the best score (GoldScore) in the normal and inverse modes were further refined using the MINIMIZE module as implemented in Sybyl, version 7.2.3 (Tripos force field and Gasteiger−Huckel charges).[16] To assess the feasibility of the inhibition mechanism, the distance between the oxygen Oγ of Ser195 and the lactone carbonyl of the coumarin ring ($O\gamma_{Ser195}$−$CO_{lactone}$) was evaluated. Furthermore, to appraise the stabilization of the compound within the S-pocket, we also measured the distance between the 5′-chlorine on the coumarin side chain and the centroid of Tyr228 aromatic ring (5′Cl−Tyr228). Such a hydrophobic contact implying a chlorine atom and Tyr228 has been shown to strengthen the interaction of **1b** with THR (observed 5′Cl−Tyr228 = 4.69 Å).[8] The obtained results are reported in Table 3.

Table 3. Computational Data

enzyme	I	mode	occurrence (%)	total energy E_T (kcal·mol^{-1})	$O\gamma_{Ser195}\cdots CO_{lactone}$ (Å)	5′Cl···Tyr228 (Å)
THR	**2b**	normal	63	−1815	2.56	3.60
		inverse	37	−1808	5.32	
	22	normal	5	−1838	2.56	3.67
		inverse	91	−1819	5.23	
α-CT	**2b**	normal	84	−1891	2.63	4.20
		inverse	14	−1870	4.42	
	22	normal	2	−1878	3.37	6.47
		inverse	29	−1866	4.46	
FXa	**2b**	normal	3	−2402	5.23	4.15
		inverse	26	−2405	5.12	
	22	normal	2	−2411	4.69	4.52
		inverse	23	−2400	5.11	
TRY	**2b**	normal	67	−512	3.38	4.20
		inverse	25	−510	4.92	
	22	normal	16	−512	3.38	4.43
		inverse	51	−511	2.99	

When **2b** is docked within the THR active site, 63% of the conformations generated by GOLD adopt the normal mode. The superposition of the first 50 solutions (Figure 1, left) emphasizes the highly conserved orientation. Key interactions stabilize the compound inside the active site (Figure 2a). The 2′,5′-dichlorophenyl is deeply inserted within the S-pocket and, similar to **1b**, interacts with Tyr228 (distance 5′Cl−Tyr228 = 3.60 Å). The coumarin ring forms a $\pi\cdots\pi$ stacking contact with Tyr60a in the P pocket (not shown in Figure 2a for clarity), while the lactone carbonyl is involved in an H-bond network with the so-called oxyanion hole (formed by the backbone NH of residues Ser195 and Gly193). In this conformation, taking into account the intrinsic flexibility of the protein,[17] a distance $O\gamma_{Ser195}$−$CO_{lactone}$ of 2.56 Å makes nucleophilic attack of Ser195 onto the coumarin ring possible and is thus consistent with the

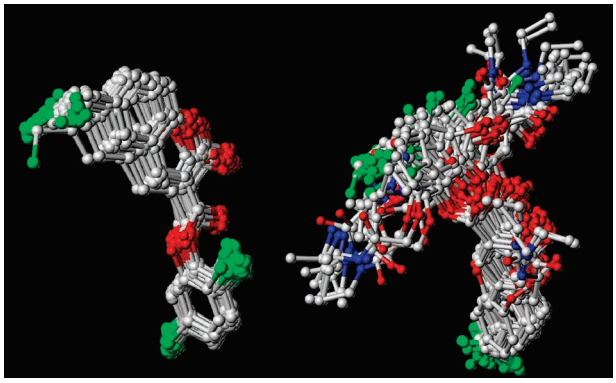

Figure 1. Superposition of the first 50 solutions generated by GOLD in the THR active site for **2b** (left) and **22** (right).

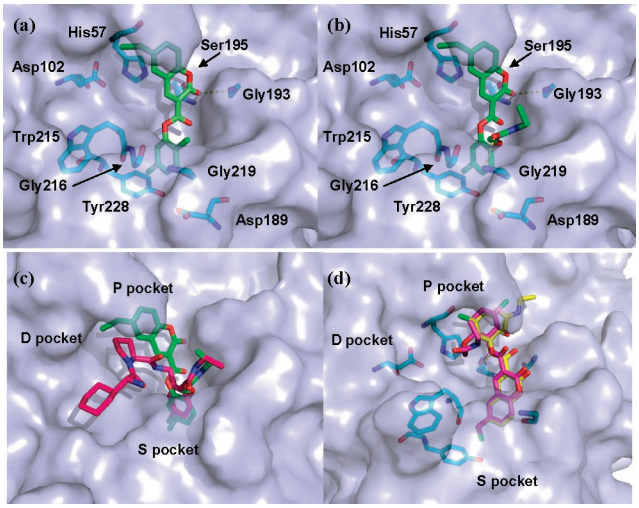

Figure 2. Normal binding mode of (a) **2b** and (b) **22** in the active site of THR. (c) Superimposition of **22** (green) and **1b** (magenta) obtained from the X-ray crystal structure (PDB code 1TA6). (d) Superimposition of both conformations obtained in the inverse mode for **22**. Pictures were made using Pymol.[18]

proposed inhibition mechanism. In contrast, in the inverse mode, the distance $O\gamma_{Ser195}-CO_{lactone}$, increased to 5.32 Å, prevents the reaction from occurring. This conformation is consequently in disagreement with the proposed mode of action of this compound. Furthermore, the difference of 7 kcal·mol^{-1} in the total energy of both complexes confirms the higher stabilization of **2b** in the normal mode compared to the inverse one.

When **22** is docked within the THR active site, only 5% of the generated conformations adopt the normal mode whereas 91% lie in the inverse one. The superposition of the first 50 conformations (Figure 1, right) does not show such a clear convergence as observed for **2b**. However, when the energy of both modes is compared, the less occurring normal orientation appears to be much more favorable than the inverse one (ΔE_T = 19 kcal·mol^{-1}).

In the normal mode, **22** is similarly to **2b** stabilized through an H-bond involving the lactone carbonyl and the oxyanion hole as well as a lipophilic $C_{aromatic}-Cl\cdots\pi$ interaction (5′Cl−Tyr228 = 3.67 Å) (Figure 2b). The distance $O\gamma_{Ser195}-CO_{lactone}$ of 2.56 Å is in agreement with the inhibition mechanism. Additionally, **22** is stabilized through an H-bond between the oxoacetamide carbonyl and the backbone NH of Gly219. A similar interaction observed in the case of **1b** crystallized with THR corroborates this binding mode.[8] Both 2-(*N*-ethyl-2′-oxoacetamide)-5′chlorophenyl side chains adopt an analogous orientation in the S-pocket, as observed in the superimposition of **1b** and **22**

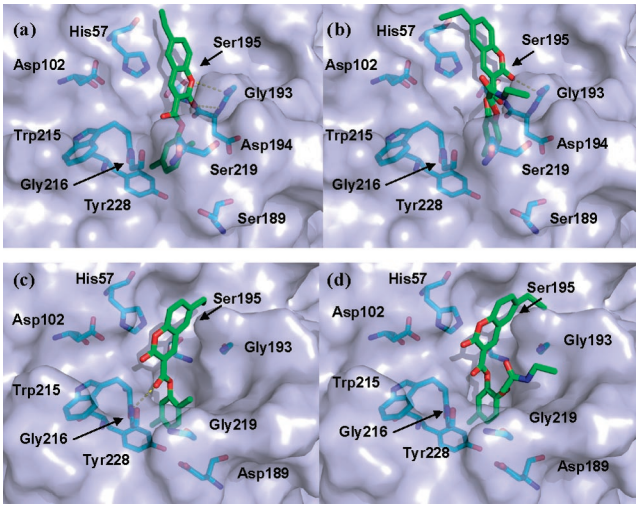

Figure 3. Docking of **2b** (left) and **22** (right) in the active site of α-CT (a, b) and FXa (c, d). Pictures were made using Pymol.[18]

(Figure 2c). The low occurrence (5%) of the normal binding mode might be partly explained by the high flexibility of the oxoacetamide side chain of **22**. Actually, many papers have reported the strong influence of ligand flexibility on the accurate prediction of binding poses, as well as the limitations of using a rigid protein during docking simulations.[19,20] However, this flexibility might also trigger the binding of **22** in the inverse orientation (Figure 2d).

In the inverse mode, two similarly occurring conformations are observed (Figure 2d), one possessing the oxoacetamide side chain on the left side (43%, in magenta) and the other on the right side (48%, in yellow) regarding the orientation of the coumarin ring. Both conformations are equally stabilized (E_T = −1819 and −1816 kcal·mol^{-1}, respectively), notably through an H-bond between the hydroxyl group of Ser195 and the O atom of the exocyclic ester. In each case, the particular orientation of the coumarin ring excludes the nucleophilic attack of Ser195 onto the lactone (distance $O\gamma_{Ser195}-CO_{lactone}$ > 5 Å). Therefore, the binding of **22** in the inverse mode prevents the inactivation of THR through the postulated inhibition mechanism. Nevertheless, in both inverse orientations, Ser195 lies in the vicinity of the exocyclic ester (distance $O\gamma_{Ser195}-CO_{exocyclic\ ester}$ = 3.5 and 3.8 Å). The nucleophilic attack of the catalytic serine onto the exocyclic carbonyl becomes achievable and might lead to the hydrolysis of the side chain, releasing the phenol and the coumarin carboxylic acid.

On the basis of these results, it can be assumed that when **22** adopts the normal orientation within the THR active site, it leads to the complete inactivation of the protein. Alternatively, the binding of **22** in the inverse mode results in a catalysis leading to its hydrolysis and the formation of side products. Therefore, the lower inhibitory activity of **22** versus **2b** could be explained by a higher decomposition rate (resulting from a binding in the inverse mode) rather than a weaker stabilization when binding in the normal orientation. The high partition ratio (k_{cat}/k_i = 13.5) experimentally observed for **22** clearly supports this hypothesis.

In α-CT, **2b** adopts again primarily the normal mode (84% of solutions), in agreement with the proposed mode of action (distance $O\gamma_{Ser195}-CO_{lactone}$ = 2.63 Å). In addition to interactions similar to those observed in THR, an H-bond occurs between the lactone carbonyl and the backbone NH of Asp194 (Figure 3a). Furthermore, the 2′-chlorine atom is surrounded by the Met192 side chain (not shown in Figure 3a for clarity; see Figure S1 in Supporting Information). This lipophilic

environment produces an extra hydrophobic stabilization of the 2′,5′-dichlorophenyl group. Together, these additional interactions might account for the high α-CT inhibitory potency observed for **2b** (k_i/K_I = 220 000 $M^{-1}\cdot s^{-1}$).

In contrast, in the case of **22** docked in α-CT, only 2% of the solutions generated adopt the normal mode (Figure 3b). Because of Met192 bordering the S-pocket, the 5′-chlorophenyl, with its bulky 2-(*N*-ethyl-2′-oxoacetamide) substituent, is clearly less deeply inserted within the cleft. Consequently, the coumarin ring, and in particular the lactone carbonyl, moves away from Ser195 (distance $O\gamma_{Ser195}-CO_{lactone}$ = 3.37 Å). Moreover, in this conformation, the lipophilic $C_{aromatic}-Cl\cdots\pi$ interaction (distance 5′Cl-Tyr228 = 6.47 Å) and the H-bond network with the oxyanion hole cannot be formed. These observations plainly explain the severe loss in the α-CT inhibitory potency for **22** vs **2b** (∼290-fold) and therefore its greatly improved selectivity profile (THR/α-CT = 5 for **22** vs 0.17 for **2b**).

For comparison purposes, we also analyzed the binding modes of **2b** and **22** within the FXa and TRY active sites. In the first protease, only 3% and 2% of the docked conformations obtained for **2b** and **22**, respectively, show the normal mode, with the 2′-substituted-5′-chlorophenyl inserted in the S-pocket (parts c and d of Figure 3, respectively). However, because of the absence of a P pocket (structural feature particular to FXa), the coumarin ring is rotated by 180°, positioning the lactone next to Gly216, far from the catalytic Ser195 (distance $O\gamma_{Ser195}-CO_{lactone}$ = 5.23 and 4.69 Å for **2b** and **22**, respectively). Therefore, whatever the substituent in the P1 position, the coumarin binds to FXa in a conformation that prevents Ser195 from reacting with the lactone moiety. This observation helps to clarify the poor inhibitory potency against this enzyme observed in all the coumarin series.[10]

In TRY, 65% of the docked solutions for **2b** exhibit the normal orientation in comparison to only 16% for **22** (Table 3). Nevertheless, in both cases, the lactone moiety is more distant from Ser195 than within the THR active site (distance $O\gamma_{Ser195}-CO_{lactone}$ = 3.38 Å) (see Supporting Information for figures). This might explain the lower inhibitory activity on TRY than on THR observed for these compounds.

Conclusion

To design selective mechanism-based inhibitors specifically targeting THR, we considered the optimization of our lead **2b**. On the basis of this parent compound, a series of new coumarins were synthesized and their biological activity assayed against THR. Among these, **22**, characterized by a 2-(*N*-ethyl-2′-oxoacetamide)-5′chlorophenyl ester moiety in the 3-position of a 6-chloromethyl-2-oxo-2*H*-1-benzopyran core, constitutes the most promising derivative. **22** is slightly less potent on THR than **2b** (THR k_i/K_I = 3455 $M^{-1}\cdot s^{-1}$ vs THR k_i/K_I = 37 000 $M^{-1}\cdot s^{-1}$), but of great interest, it exhibits a drastically improved selectivity profile, particularly regarding α-CT (selectivity ratios of 58, 29, and 5 for FXa, TRY, and α-CT, respectively). As shown by molecular docking, the bulky 2-(*N*-ethyl-2′-oxoacetamide) chain prevents suitable orientation of the coumarin nucleus in the α-CT active site for the required nucleophilic attack by the active Ser195.

To our knowledge, such selectivity has never been reported previously in mechanism-based THR inhibitors deprived of a basic moiety. **22** thus represents a remarkable pharmacological tool to further explore selective mechanism-based THR inhibitors.

Experimental Section

Detailed synthesis of intermediates **4**−**7**, **9**−**11**, **13**−**15** and the targeted compounds **21**−**29** can be found in the Supporting Information.

(2-Hydroxy-4-chlorophenoxy)-*N*-ethylacetamide (11). To a solution of ethyl 2-methoxy-4-chlorophenoxyacetate **9** (1 g, 4.1 mmol) in CH_2Cl_2 (10 mL) is added a solution of BBr_3 prepared from 1.46 g of BBr_3 (5.5 mmol) diluted in dry CH_2Cl_2 (5.55 mL). The mixture is vigorously stirred for 1 h at room temperature. After this time, the solvents are removed and the residue is dissolved in CH_2Cl_2 (30 mL), washed with water and brine, dried over $MgSO_4$, and evaporated to dryness. The crude product is purified by column chromatography (eluant, 100% AcOEt) to afford 420 mg (1.99 mmol) of pure 2-hydroxy-4-chlorophenoxyacetic acid **10** (yield, 47%). Then, to a solution of **10** (300 mg, 1.48 mmol), hydroxybenzotriazole (HOBT) (220 mg, 1.63 mmol), ethylamine chlorhydrate (133 mg, 1.63 mmol), and *N*-methylmorpholine (NMM) (330 mg, 3.26 mmol) in dry DMF (10 mL) is added the ethyl-3-(3-(dimethylamino)propyl)carbodiimide chlorhydrate (EDC) (340 mg, 1.77 mmol). The mixture is stirred for 18 h under an inert atmosphere and then diluted by AcOEt (50 mL), washed with water (3 × 50 mL) and brine, dried over $MgSO_4$, and evaporated. The crude product is purified by chromatography column (eluant, AcOEt 100%) to give 290 mg (1.26 mmol) of the desired **11** (yield, 86%).

General Method for the Synthesis of Compounds 21−29.[10] To a flask containing 1 g (4.54 mmol) of 6-hydroxymethyl-2-oxo-2*H*-chromene-3-carboxylic acid is added thionyl chloride (10 mL). This solution is refluxed for 3 h under an argon atmosphere. After cooling, the mixture is evaporated and dry toluene (10 mL) is added to the residue and evaporated. This operation is repeated three times. Then, to the dried acyl chloride dissolved in dry dioxane (20 mL) are added the required alcohol or amine (1.1 equiv) and dry pyridine (1.1 equiv). After 2 h, the solvents are evaporated and the residue is dissolved in AcOEt (150 mL) and washed three times with 0.1 N HCl (50 mL). The combined organic phases are dried over $MgSO_4$ and evaporated to dryness. The final compounds are purified by crystallization (acetonitrile, **21**; AcOEt, **24**−**29**), preparative HPLC (**22**), or collected filtration (**23**).

Acknowledgment. C.C. is greatly indebted to the Belgian National Foundation for Scientific Research (FNRS) for the award of a research fellowship.

Supporting Information Available: Detailed description of the synthesis of **21**−**29** and intermediates **4**−**7, 9**−**11**, **13**−**15**, molecular modeling methods, biological assays, mass spectra, and analytical data of all compounds. This material is available free of charge via the Internet at http://pubs.acs.org.

References

(1) Hirsh, J.; O'Donnell, M.; Weitz, J. I. New anticoagulants. *Blood* **2005**, *105* (2), 453−463.
(2) Weitz, J. I. New anticoagulants for treatment of venous thromboembolism. *Circulation* **2004**, *110* (9), I19−I26.
(3) De Simone, G.; Menchise, V.; Omaggio, S.; Pedone, C.; Scozzafava, A.; Supuran, C. T. Design of weakly basic thrombin inhibitors incorporating novel P1 binding functions: molecular and X-ray crystallographic studies. *Biochemistry* **2003**, *42* (30), 9013−9021.
(4) Lumma, W. C., Jr.; Witherup, K. M.; Tucker, T. J.; Brady, S. F.; Sisko, J. T.; Naylor-Olsen, A. M.; Lewis, S. D.; Lucas, B. J.; Vacca, J. P. Design of novel, potent, noncovalent inhibitors of thrombin with nonbasic P-1 substructures: rapid structure−activity studies by solid-phase synthesis. *J. Med. Chem.* **1998**, *41* (7), 1011−1013.
(5) Sanderson, P. E.; Stanton, M. G.; Dorsey, B. D.; Lyle, T. A.; McDonough, C.; Sanders, W. M.; Savage, K. L.; Naylor-Olsen, A. M.; Krueger, J. A.; Lewis, S. D.; Lucas, B. J.; Lynch, J. J.; Yan, Y. Azaindoles: moderately basic P1 groups for enhancing the selectivity of thrombin inhibitors. *Bioorg. Med. Chem. Lett* **2003**, *13* (5), 795−798.
(6) Scozzafava, A.; Briganti, F.; Supuran, C. T. Protease inhibitors. Part 3. Synthesis of non-basic thrombin inhibitors incorporating pyridinium-sulfanilylguanidine moieties at the P1 site. *Eur. J. Med. Chem.* **1999**, *34* (11), 939−952.

(7) Supuran, C. T.; Scozzafava, A.; Briganti, F.; Clare, B. W. Protease inhibitors: synthesis and QSAR study of novel classes of nonbasic thrombin inhibitors incorporating sulfonylguanidine and *O*-methylsulfonylisourea moieties at P1. *J. Med. Chem.* **2000**, *43* (9), 1793−1806.
(8) Tucker, T. J.; Brady, S. F.; Lumma, W. C.; Lewis, S. D.; Gardell, S. J.; Naylor-Olsen, A. M.; Yan, Y.; Sisko, J. T.; Stauffer, K. J.; Lucas, B. J.; Lynch, J. J.; Cook, J. J.; Stranieri, M. T.; Holahan, M. A.; Lyle, E. A.; Baskin, E. P.; Chen, I. W.; Dancheck, K. B.; Krueger, J. A.; Cooper, C. M.; Vacca, J. P. Design and synthesis of a series of potent and orally bioavailable noncovalent thrombin inhibitors that utilize nonbasic groups in the P1 position. *J. Med. Chem.* **1998**, *41* (17), 3210−3219.
(9) Pochet, L.; Doucet, C.; Schynts, M.; Thierry, N.; Boggetto, N.; Pirotte, B.; Jiang, K. Y.; Masereel, B.; de Tullio, P.; Delarge, J.; Reboud-Ravaux, M. Esters and amides of 6-(chloromethyl)-2-oxo-2*H*-1-benzopyran-3-carboxylic acid as inhibitors of alpha-chymotrypsin: significance of the "aromatic" nature of the novel ester-type coumarin for strong inhibitory activity. *J. Med. Chem.* **1996**, *39* (13), 2579−2585.
(10) Frederick, R.; Robert, S.; Charlier, C.; de Ruyck, J.; Wouters, J.; Pirotte, B.; Masereel, B.; Pochet, L. 3,6-Disubstituted coumarins as mechanism-based inhibitors of thrombin and factor Xa. *J. Med. Chem.* **2005**, *48* (24), 7592−7603.
(11) Silverman, R. B. Mechanism-based enzyme inactivators. *Methods Enzymol.* **1995**, *249*, 240−283.
(12) Doucet, C.; Pochet, L.; Thierry, N.; Pirotte, B.; Delarge, J.; Reboud-Ravaux, M. 6-Substituted 2-oxo-2*H*-1-benzopyran-3-carboxylic acid as a core structure for specific inhibitors of human leukocyte elastase. *J. Med. Chem.* **1999**, *42* (20), 4161−4171.
(13) Pochet, L.; Doucet, C.; Dive, G.; Wouters, J.; Masereel, B.; Reboud-Ravaux, M.; Pirotte, B. Coumarinic derivatives as mechanism-based inhibitors of alpha-chynotrypsin and human leukocyce elastase. *Bioorg. Med. Chem.* **2000**, *8* (6), 1489−1501.
(14) Pochet, L.; Dieu, M.; Frédérick, R.; Murray, A. M.; Kempen, I.; Pirotte, B.; Masereel, B. Investigation of the inhibition mechanism of coumarins on chymotrypsin by mass spectrometry. *Tetrahedron* **2003**, *59*, 4557−4561.
(15) Jones, G.; Willett, P.; Glen, R. C.; Leach, A. R.; Taylor, R. Development and validation of a genetic algorithm for flexible docking. *J. Mol. Biol.* **1997**, *267* (3), 727−748.
(16) *Sybyl*, version 7.2.3; Tripos Inc. (1699 South Hanley Rd, St. Louis, MO, 63144).
(17) Teague, S. J. Implications of protein flexibility for drug discovery. *Nat. Rev. Drug Discovery* **2003**, *2* (7), 527−541.
(18) DeLano, W. L. *The PyMOL Molecular Graphics System*; DeLano Scientific: San Carlos, CA, 2002.
(19) Perola, E.; Walters, W. P.; Charifson, P. S. A detailed comparison of current docking and scoring methods on systems of pharmaceutical relevance. *Proteins* **2004**, *56* (2), 235−249.
(20) Erickson, J. A.; Jalaie, M.; Robertson, D. H.; Lewis, R. A.; Vieth, M. Lessons in molecular recognition: the effect of ligand and protein flexibility on molecular docking accuracy. *J. Med. Chem.* **2004**, *47*, 45−55.

JM061368V